

Adatom formation mechanism on Ag(110) studied by quasielastic He atom scattering

L. Pedemonte* and G. Bracco

Istituto Nazionale di Fisica della Materia and IMEM-CNR, Dipartimento di Fisica dell'Università di Genova, Via Dodecaneso 33, 16146 Genova, Italy

(Received 30 May 2003; published 20 November 2003)

The temperature dependence of the diffuse elastic peak is measured using helium atom scattering on Ag(110) along the $\langle 1\bar{1}0 \rangle$ azimuth. A previous study performed by our group [Phys. Rev. B **66**, 45 414 (2002)] demonstrates that this scattering contribution may be ascribed to silver atoms adsorbed on the flat (110) terraces. To obtain information on the adatom creation process the evolution of the peak intensity is analyzed following the method proposed by Silvestri, Graham, and Toennies [Phys. Rev. Lett. **81**, 1034 (1998)]. In the case of Ag(110) this method has to be modified to take into account the anharmonic contributions to the surface lattice vibrations. The energy for adatom formation is determined to be $E_a = (0.38 \pm 0.03)$ eV. This estimate is compared with the predictions of molecular-dynamics simulations suggesting that adatoms are mainly released from flat terraces and/or from $\langle 1\bar{1}0 \rangle$ oriented step edges.

DOI: 10.1103/PhysRevB.68.205420

PACS number(s): 68.43.De, 68.47.De, 68.35.Ja

I. INTRODUCTION

Surface diffusion of adsorbed atoms and molecules plays a key role in most dynamical processes occurring on crystal faces such as chemical reactions, growth of thin film and of epitaxial layers, morphological equilibration of two-dimensional nanostructures, etc.¹⁻³ The knowledge of the microscopic mechanisms which govern adparticle diffusion is therefore of great interest from a fundamental point of view and for many technological applications. In the past years diffusion on metal and semiconductor surfaces has been extensively studied both experimentally and theoretically⁴⁻⁶ and self-diffusion on the (110) face of fcc crystals has attracted the attention of the researchers because of its anisotropy leading, among other interesting features, to a rich variety of nanostructures during sputtering and growth.⁷ In the case of Ag(110), elementary diffusion processes have been described using molecular dynamics (MD).⁸ In particular, adatom diffusion on the flat (110) terraces is demonstrated to be easy along the $\langle 1\bar{1}0 \rangle$ atomic channels where jumping between first neighbor absorption sites is suggested as the main diffusion mechanism. Along the cross-channel $\langle 001 \rangle$ direction self-diffusion is proved to be more difficult and to occur preferably by exchange. From the experimental point of view, strong anisotropic surface diffusion is indicated as a key ingredient to understand the results of scanning tunnel microscopy (STM) measurements of Ag/Ag(110) on the grow and the decay of islands in the temperature range between 155 and 300 K.⁹⁻¹¹ Anisotropic energy barriers are also observed to play a crucial role in the morphological equilibration of rippled nanostructures below 250 K.^{12,13} These low-temperature experiments have been recently extended by the quasielastic helium atom scattering (QHAS) study performed by our group.¹⁴⁻¹⁶ Briefly, self-diffusion on the Ag(110) surface has been investigated in the temperature range up to 800 K. Adatom jumping along the $\langle 1\bar{1}0 \rangle$ surface channels is detected above 600 K while along the $\langle 001 \rangle$ azimuth diffusion is observed above 750 K. The effective energy barrier for jumping is measured and good

agreement is obtained with the adiabatic value calculated by MD.

Although the above mentioned studies provide a quite satisfactory picture of self-diffusion on Ag(110) a fundamental step in understanding this process is to study how the moving adatoms are created. In this regard, we recall that the (110) face of silver is well known to develop a rich phenomenology on increasing the sample temperature. For instance, an STM study suggests that the step edges which bound (110) terraces start to meander above 500 K.¹⁷ At the very same temperature, low-energy ion scattering (LEIS) measurements show an extra increase of the mean vibration amplitude of the surface lattice^{18,19} which accompanies the onset of surface roughening at 600 K.²⁰⁻²² Whenever the vibration amplitude of the topmost layer atoms is enhanced some of them overcome the potential barrier giving rise to vacancies/adatoms on the surface. A few percent of vacancies is detected at temperatures slightly above 700 K with LEIS (Ref. 19) in good agreement with the results of MD calculations.^{23,24} A method to determine the energy of an atom adsorbed on the surface has been introduced by Silvestri, Graham, and Toennies (SGT) in Ref. 25. There, the evolution with temperature of the quasielastic peak scattered from the Ni(110) surface is analyzed but a greater adatom formation energy is obtained than predicted by calculations.²⁶ The results of SGT have been further questioned by Theis who has suggested that the observed scattering contribution is not due to adatoms but is most likely caused by steps.^{27,28} In order to gain a deeper insight into the mechanism of adatom formation as well as to contribute to the discussed topic, we present a set of quasielastic helium scattering measurements performed on the (110) surface of silver. The motivation to repeat the SGT analysis is given by our previous QHAS results which demonstrate that the quasielastic intensity diffused along the $\langle 1\bar{1}0 \rangle$ surface channels above 600 K has to be ascribed to silver adatoms diffusing on the surface.¹⁴⁻¹⁶ Moreover, while the SGT analysis assumes harmonic lattice vibrations, we show that surface anharmonicity has to be taken into account to obtain a reli-

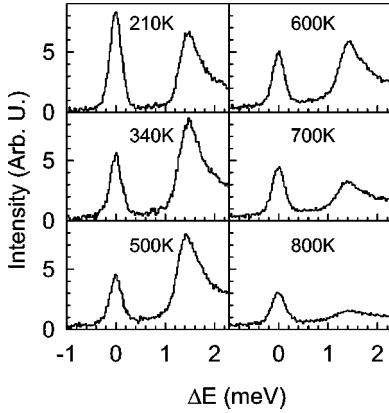


FIG. 1. Energy converted time-of-flight spectra for He scattered from Ag(110) along the $\langle 1\bar{1}0 \rangle$ azimuthal direction at increasing surface temperature. The beam energy is $E=7.3$ meV, the incident and the total scattering angle are $\theta_i=60.7^\circ$ and $\theta_t=110^\circ$, respectively. Within this geometry the parallel momentum transfer yields $\Delta K=0.43 \text{ \AA}^{-1}$.

able estimate of the energy for adatom formation on Ag(110).

The paper is organized as follows. Section II describes the experimental details, while the data and the analysis are presented in Sec. III. Finally, in Sec. IV conclusions are made.

II. EXPERIMENT

Measurements are performed by means of the custom-built He atom scattering apparatus with time-of-flight (TOF) detection system described in detail elsewhere.²⁹ Briefly, the supersonic He nozzle beam is produced at source temperature $T_0=36$ K and pressure $P_0=5$ bar with most probable energy of about $E=7.32$ meV corresponding to wave vector $k=3.76 \text{ \AA}^{-1}$. The beam velocity spread results in $\Delta v/v < 1\%$. Before interacting with the sample, the beam is chopped into short pulses of a few microseconds of duration by a rotating slotted disk. Then, the scattered fraction is differentially pumped, ionized, and mass selected at fixed total deflection angle $\theta_t=110^\circ$. The incident angle θ_i and the scattering angle θ_f refer to the surface normal and are changed simultaneously by rotating the sample. The chopper to sample and the sample to ionizer distances are ~ 73 mm and ~ 728 mm, respectively. The base pressure of the scattering chamber is in the 10^{-11} mbar range. The Ag specimen, spark cut from a single crystal ingot and chemomechanically polished in the (110) orientation within 0.2° , is cleaned in ultrahigh vacuum by Ar-ion sputtering and annealing cycles until the usual diffraction pattern is obtained. The full width at half maximum of the specular peak measured on a well prepared sample provides an estimate of the scattering coherence length of about 700 \AA . The crystal temperature T is measured by a K -type thermocouple with reproducibility within 5 K and accuracy ± 15 K.

III. RESULTS AND DATA ANALYSIS

Figure 1 shows typical energy-converted TOF spectra measured at crystal temperatures between 210 and 800 K

along the $\langle 1\bar{1}0 \rangle$ azimuthal direction. The spectra are obtained at parallel momentum transfer $\Delta K=0.43 \text{ \AA}^{-1}$ corresponding to $\sim 40\%$ of the Brillouin zone boundary. Here, no elastic scattered intensity is expected from a perfect periodic surface since the parallel momentum is conserved to within a reciprocal lattice vector. However, the defects on a real crystal (steps and adatoms) scatter some of the helium atoms incoherently giving rise to the peak at $\Delta E=0$, the so called quasielastic peak. In addition, an inelastic feature is observed at approximately 1.4 meV which can be identified as the sum of contributions from the Rayleigh mode and the MS_0 singularity of the phonon spectrum.³⁰ It can be noted that the intensity of the quasielastic peak follows a nonmonotonic behavior on increasing the sample temperature. In fact, it decreases by about a factor 2 between 210 and 500 K, then it slightly increases at 600 K, and it is finally dramatically reduced at 800 K.

It is worthwhile to recall here that at fixed scattering conditions and at low defect density, n , the intensity of the quasielastic structure is proportional to the concentration of surface defects. Furthermore, the peak intensity is reduced with increasing temperature by the Debye-Waller (DW) factor, $2W$, so that³¹

$$I \propto n \exp(-2W). \quad (3.1)$$

Within the present scattering geometry the DW factor reduces with very little approximation to its value at the specular angle

$$2W = \Delta k_z^2 \langle u_z^2 \rangle, \quad (3.2)$$

where $\langle u_z^2 \rangle$ is the mean-square vibration amplitude of the topmost layer atoms perpendicular to the surface plane and Δk_z is the perpendicular momentum transfer. In the case of atom-surface scattering the overall expression of the Debye-Waller factor introduced by Eq. (3.1) and Eq. (3.2) is expected to be valid for a beam of fast light particles which collides with a hard surface made by heavy atoms and showing a negligible attractive well.³² Whenever these restrictions are relaxed corrections have been proposed to account for several effects. First, collisions may have characteristic times comparable to those of lattice vibrations.³² Moreover, the incident atoms may interact simultaneously with several surface scatterers³³ and are accelerated toward the surface by the attractive potential well (Beeby effect).³⁴ The last effect often provides the most relevant correction in the experiments carried out with light helium atoms³⁵ and is taken into account by substituting Δk_z in Eq. (3.2) with the effective perpendicular momentum transfer

$$\Delta k_{z(e)} = k \{ \sqrt{[\cos(\theta_f)]^2 + D/E} + \sqrt{[\cos(\theta_i)]^2 + D/E} \},$$

D being the average well depth. In Ref. 25 the harmonic Debye model is adopted to describe the lattice vibrations so that

$$\langle u_z^2 \rangle_{\text{harm}} = \frac{3\hbar^2 T}{M k_b \Theta_D}$$

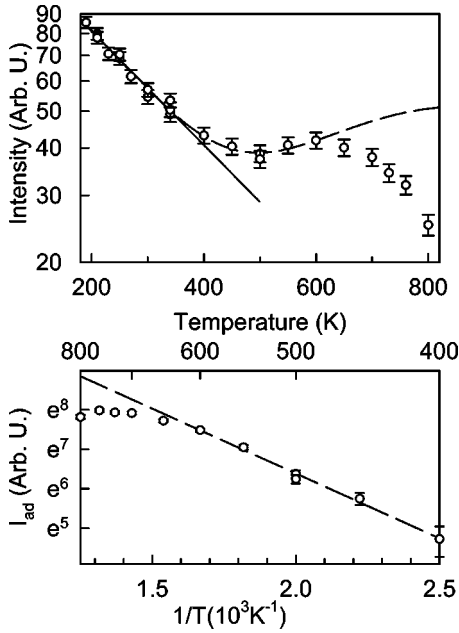


FIG. 2. In the upper panel the intensity of the quasielastic peak measured as a function of the surface temperature T is reported on a log scale using open symbols. At $T \leq 350$ K the intensity decrease due to the harmonic Debye-Waller attenuation is described by the best-fit solid straight line. The dashed line is the best-fit curve through the data at $T \leq 600$ K obtained using Eq. (3.3). In the lower panel, the Arrhenius plot of the DW corrected adatom contribution to the scattered intensity, I_{ad} , is shown. The dashed straight line corresponds to the dashed curve in the upper panel and its slope yields an estimate of the energy for adatom formation of ~ 0.28 eV.

with k_b the Boltzmann constant, M the mass of the target atoms, and Θ_D the surface Debye temperature. The corresponding DW factor is

$$2W = \Delta k_{z(e)}^2 \frac{3\hbar^2 T}{Mk_b \Theta_D} = C_{DW} T.$$

The SGT analysis further assumes that the density of defects is the sum of two contributions: static defects (steps) having constant concentration on increasing temperature and thermally activated defects, i.e., mainly adatoms. Hence,

$$I = [I_{st} + I_{ad}^0 \exp(-E_a/k_b T)] \exp(-C_{DW} T), \quad (3.3)$$

where E_a is the energy for the creation of an adatom, I_{st} and I_{ad}^0 are constants proportional to the step and adatom density, respectively. Using Eq. (3.3) it is possible to determine the evolution with temperature of the adatom density from the quasielastic peak intensity if the effect of the Debye-Waller contribution is taken into account.

To this aim, we have measured the evolution of I by fitting the quasielastic peaks collected in the temperature range between 190 and 800 K as the sum of a Voigt function with a linear background. The amplitude of the best-fit Voigt curve is reported on log scale as a function of temperature in the upper panel of Fig. 2. It can be noted that the exponential decay law predicted in the low-temperature range by Eq. (3.3) is well satisfied below ~ 350 K. In particular, the slope

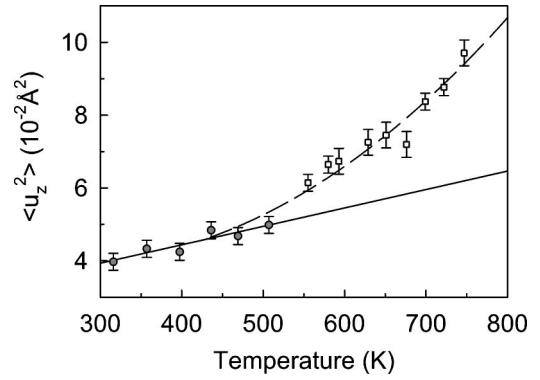


FIG. 3. Symbols illustrate the evolution with temperature of the perpendicular mean-square vibration amplitude of the topmost layer atoms, $\langle u_z^2 \rangle$, measured using low-energy ion scattering spectroscopy (see Ref. 19 for more details). The data up to approximately 530 K (filled circles) are fitted by the continuous straight line expected for the Debye model. At higher temperatures symbols (open squares) follow the best-fit quadratic dashed curve.

C_{DW} of the corresponding best fit straight line provides an estimate of the surface Debye temperature of $\Theta_D = (185 \pm 18)$ K. This value is obtained taking into account the Beeby correction for the He-Ag(110) interaction with $D = 6.0$ eV.³⁶ The static defect contribution I_{st} is further obtained as best-fit parameter corresponding to the scattered intensity at $T = 0$ K. Above 350 K deviations from the Debye behavior are observed due to the creation of thermally activated defects. To isolate the adatom contribution,

$$I_{ad} = I_{ad}^0 \exp(-E_a/k_b T),$$

the harmonic DW term is factored out and the constant I_{st} is subtracted from the data. The results are reported on an Arrhenius plot in the lower panel of Fig. 2. Here, I_{ad} is observed to follow the linear behavior predicted by Eq. (3.3) up to ~ 600 K, hence a strong deviation sets in. A least-squares fit of Eq. (3.3) to the intensities in the temperature range 190–600 K is reported in the upper panel as a dashed curve and the corresponding adsorbate contribution is shown in the lower panel as dashed line. The inferred value for the adatom creation energy is $E_a = (0.28 \pm 0.02)$ eV. This value appears quite small in comparison to the MD estimate of ~ 0.38 eV for the formation energy of a vacancy-adatom pair on a flat (110) terrace.³⁷

In order to resolve the discrepancy and to explain the deviation from the Arrhenius behavior the SGT analysis has been further developed. In particular, Fig. 3 reports the evolution versus temperature of the Ag(110) mean-square vibration amplitude measured by our group using LEIS. The data are described in detail in Ref. 19. Here, it is helpful to recall that within the scattering geometry of that experiment the perpendicular component of the surface atom displacement is measured. The figure shows that $\langle u_z^2 \rangle$ follows the linear behavior expected for the Debye model up to approximately 530 K. The Debye temperature estimated in the range 300–530 K is $\Theta_D = (163 \pm 15)$ K in good agreement with the present QHAS value. Above 530 K the lattice vibrations become anharmonic and the lattice vibration amplitude is

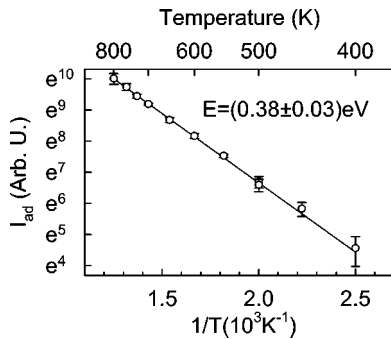


FIG. 4. Arrhenius plot of I_{ad} obtained from Eq. (3.4). The slope of the best-fit solid line provides an energy for adatom formation of (0.38 ± 0.03) eV.

strongly enhanced. In order to account for the enhancement of $\langle u_z^2 \rangle$ the analysis of the quasielastic data has been modified by introducing in the DW factor of Eq. (3.3) a temperature dependent term, $f(T) = \langle u_z^2 \rangle / \langle u_z^2 \rangle_{harm}$, that is

$$I = [I_{st} + I_{ad}^0 \exp(-E_a/k_b T)] \exp[-C_{DW} f(T) T]. \quad (3.4)$$

Of course, $f(T) = 1$ for $T < 530$ K. In the range 550–800 K, $f(T)$ is estimated using the LEIS results. In detail, the evolution of $\langle u_z^2 \rangle$ is described by the best-fit parabolic curve reported as dashed line in Fig. 3. At a given temperature, f is obtained as the ratio between the observed mean-square displacement and the corresponding harmonic value estimated along the low-temperature best-fit straight line. Following Eq. (3.4) the DW term corrected for surface anharmonicity is factored out from the quasielastic intensity and the constant I_{st} is subtracted to isolate the adatom contribution. The corresponding results are reported versus temperature on the Arrhenius plot of Fig. 4. Note that I_{ad} now follows the Arrhenius law over the whole temperature range. Moreover, an estimate of the energy for adatom formation provides $E_a = (0.38 \pm 0.03)$ eV in very good agreement with the predictions of MD simulations.³⁷

IV. DISCUSSION AND CONCLUSIONS

In the preceding section the evolution with temperature of the intensity of the quasielastic peak obtained from the Ag(110) surface is studied to determine the onset of the adatom detachment and the energy of this process. In the temperature range between 190 and 350 K the scattering contribution from static defects predominates and the peak intensity is observed to decrease exponentially with T because of the DW harmonic attenuation. The value of (185 ± 18) K obtained for the Debye temperature appears slightly larger than the previous theoretical and experimental estimates.^{38,39} However, it fits well with the LEIS results reported in Sec. III (Ref. 19) and is also in the range of the standard estimate that Θ_D is about $1/\sqrt{2}$ of the bulk Debye temperature (~ 165 K).⁴⁰

Above 350 K deviations from the DW behavior are observed due to thermal induced defects. In order to describe the evolution of the scattered intensity over the temperature range up to 800 K the analysis discussed by Silvestri, Gra-

ham, and Toennies²⁵ has to be modified to include surface anharmonicity. To this end, an *ad hoc* temperature-dependent term is introduced in the harmonic Debye-Waller factor. This is of course a very rough approximation; however, a rigorous expression of the DW term in atom-surface scattering, though studied by many theoreticians, is at present still not available.⁴¹ The evolution versus T of the mean-square vibration amplitude of the topmost layer atoms is estimated using a parabolic approximation of the LEIS measurements. As the functional form of the curve adopted to describe the data is to a large extent arbitrary we have carefully checked that different choices of the best-fit function would not alter the results of the preceding section. For instance, using a linear approximation of $\langle u_z^2 \rangle$ at $T \geq 550$ K the adsorbate intensity is observed to follow an Arrhenius behavior similar to that reported in Fig. 4. The corresponding energy is about 1.5% greater than the present value of 0.38 eV. A further attempt has been performed to estimate the anharmonic contribution to the surface lattice vibrations using the MD predictions discussed in Ref. 23. In that case, I_{ad} recovers the Arrhenius behavior in the temperature range between 400 and 600 K with $E_a \sim 0.32$ eV. However, at higher temperatures strong deviations are observed suggesting an overestimate of $\langle u_z^2 \rangle$. It is worthwhile to remark here that whenever surface anharmonicity is included in the DW term the scattering contribution due to the thermally activated defects rapidly overwhelms the contribution from static defects. The latter constitutes at 600 K only 30% of the total scattered intensity and decreases down to a few percent at 800 K. Furthermore, the thermal defects are observed to diffuse above 600 K. In fact, a broadening of the quasielastic peak is detected which attains the value of ~ 60 μ eV at 800 K. These results fully agree with our previous QHAS studies^{14–16} and definitively exclude the possibility that the evolution with temperature of the quasielastic scattered intensity has to be mainly ascribed to an increase of the total step length as suggested by Theis for the Ni(110) case.²⁷

Concerning the experimental value of $E_a = (0.38 \pm 0.03)$ eV it shows very good agreement with the MD prediction of $E_{va} = 0.38$ eV for the energy of a vacancy-adatom pair on the flat Ag(110) terrace.³⁷ This value is obtained by modeling silver by a semiempirical potential and taking into account the full environment of the atom both in the initial and in the final state of the process.⁸ However, the description of the (110) surface can be safely simplified if the anisotropic bond-breaking model is adopted.¹² Within this model $E_{va} = 0.40$ eV corresponds to the energy required to break two strong in-channel bonds and two weak cross-channel bonds, having a strength of ~ 0.18 eV and 0.02 eV, respectively. The energies needed to detach an atom from a close-packed $\langle 1\bar{1}0 \rangle$ oriented step and from a loose $\langle 001 \rangle$ oriented step can be further calculated to be $E_{\langle 1\bar{1}0 \rangle} = 0.38$ eV and $E_{\langle 001 \rangle} = 0.22$ eV. These estimates indicate that within the accuracy of the experiment we cannot distinguish if the adatoms predominantly come out from the (110) terraces or from the close-packed step edges. Moreover, although $E_{\langle 001 \rangle}$ is the lowest energy the corresponding process provides only a secondary contribution to the adatom den-

sity. To explain this result we suggest that the surface steps are mainly oriented along the $\langle 1\bar{1}0 \rangle$ direction over the whole temperature range considered here, i.e., a negligible concentration of loose steps is expected. This picture is well supported by the results of STM studies on Ag(110) where straight monoatomic steps running preferentially along the $\langle 1\bar{1}0 \rangle$ rows are seen at 300 K.^{17,42,43} On increasing the temperature the steps are observed to meander by kink movement and to release atoms to the underlying terraces. Anisotropic *missing row* defects, i.e., $\langle 1\bar{1}0 \rangle$ rows or pieces of them which are missing, are detected by LEIS within the fringed region near step edges in the temperature range up to 900 K,¹⁹ in good agreement with the theoretical predictions.⁴⁴ Above 700 K LEIS measurements also point out an increasing percentage of vacancies in the topmost surface layer suggesting that at the highest temperatures both the step edges and the flat terraces are effective in releasing atoms to the silver surface.

In summary, we have demonstrated that the SGT method can provide a reasonable picture of the adatom creation pro-

cess on Ag(110) provided that the anharmonic contributions to the topmost layer vibration amplitude are taken into account. In particular, the evolution with temperature of the Debye-Waller corrected intensity, I_{ad} , shows that the adatom detachment is a thermally activated process with an energy of 0.38 eV. Though this estimate is obtained using a very simple model its value compares well with the predictions of the MD simulations suggesting that both the $\langle 1\bar{1}0 \rangle$ oriented step edges and the flat (110) terraces play an important role in the creation of adatoms.

ACKNOWLEDGMENTS

The work was supported by the Italian MIUR through Grant No. 2001021128. Dr. Professor W. Heiland and Dr. K. Brüning are gratefully acknowledged for taking part in the LEIS measurements. Fruitful discussions with Dr. R. Ferrando and Professor R. Tatarek are also acknowledged. Last but not least, the authors thank A. Gussoni for technical assistance.

*Electronic address: pedemont@fisica.unige.it

- ¹A. Pimpinelli and J. Villain, *Physics of Crystal Growth* (Cambridge University Press, Cambridge, 1998).
- ²A.L. Barabási and H.E. Stanley, *Fractal Concepts in Surface Growth* (Cambridge University Press, Cambridge, 1995).
- ³K. Morgenstern, E. Laegsgaard, I. Stensgaard, F. Besenbacher, M. Bohringer, W.D. Schneider, R. Berndt, F. Mauri, A. De Vita, and R. Car, *Appl. Phys. A: Mater. Sci. Process.* **69**, 559 (1999).
- ⁴T. Ala Nissila, R. Ferrando, and S.C. Ying, *Adv. Phys.* **51**, 949 (2002).
- ⁵A.G. Naumovets and Z. Zhang, *Surf. Sci.* **500**, 414 (2002).
- ⁶A.P. Jardine, J. Ellis, and W. Allison, *J. Phys.: Condens. Matter* **14**, 6173 (2002).
- ⁷U. Valbusa, C. Boragno, and F. Buatier de Mongeot, *J. Phys.: Condens. Matter* **14**, 8153 (2002), and references therein.
- ⁸F. Hontinfinde, R. Ferrando, and A.C. Levi, *Surf. Sci.* **366**, 306 (1996).
- ⁹S. Rusponi, C. Boragno, R. Ferrando, F. Hontinfinde, and U. Valbusa, *Surf. Sci.* **440**, 451 (1999).
- ¹⁰C. de Giorgi, P. Aihemaiti, F. Buatier de Mongeot, C. Boragno, R. Ferrando, and U. Valbusa, *Surf. Sci.* **487**, 49 (2001).
- ¹¹K. Morgenstern, E. Laegsgaard, I. Stensgaard, and F. Besenbacher, *Phys. Rev. Lett.* **83**, 1613 (1999).
- ¹²A. Videcoq, F. Hontinfinde, and R. Ferrando, *Surf. Sci.* **515**, 575 (2002).
- ¹³L. Pedemonte, G. Bracco, C. Boragno, F. Buatier de Mongeot, and U. Valbusa, *Phys. Rev. B* **68**, 115431 (2003).
- ¹⁴L. Pedemonte, R. Tatarek, and G. Bracco, *Surf. Sci.* **502/503**, 341 (2002).
- ¹⁵L. Pedemonte, R. Tatarek, M. Vladiskovic, and G. Bracco, *Surf. Sci.* **507/510**, 129 (2002).
- ¹⁶L. Pedemonte, R. Tatarek, and G. Bracco, *Phys. Rev. B* **66**, 45 414 (2002).
- ¹⁷R. Koch, J.J. Schulz, and K.H. Rieder, *Europhys. Lett.* **48**, 554 (1999).
- ¹⁸L. Pedemonte, R. Tatarek, M. Aschoff, K. Brüning, and W.

- Heiland, *Nucl. Instrum. Methods Phys. Res. B* **164/165**, 645 (2000).
- ¹⁹L. Pedemonte, R. Tatarek, M. Aschoff, K. Brüning, and W. Heiland, *Surf. Sci.* **482/485**, 1457 (2001).
- ²⁰G. Bracco, C. Malò, C.J. Moses, and R. Tatarek, *Surf. Sci.* **287/288**, 687 (1993).
- ²¹G. Bracco, L. Bruschi, R. Tatarek, A. Franchini, V. Bortolani, and G. Santoro, *Europhys. Lett.* **34**, 687 (1996).
- ²²G. Bracco, L. Pedemonte, and R. Tatarek, *Phys. Rev. B* **54**, 10 385 (1996).
- ²³T.S. Rahman and Z.J. Tian, *J. Electron Spectrosc. Relat. Phenom.* **64/65**, 651 (1993).
- ²⁴T.S. Rahman, Z.J. Tian, and J.E. Black, *Surf. Sci.* **374**, 9 (1997).
- ²⁵W. Silvestri, A.P. Graham, and J.P. Toennies, *Phys. Rev. Lett.* **81**, 1034 (1998).
- ²⁶W. Silvestri, A.P. Graham, and J.P. Toennies, *Phys. Rev. Lett.* **83**, 5183 (1999).
- ²⁷W. Theis, *Phys. Rev. Lett.* **84**, 2038 (2000).
- ²⁸W. Silvestri, A.P. Graham, and J.P. Toennies, *Phys. Rev. Lett.* **84**, 2039 (2000).
- ²⁹L. Pedemonte, A. Gussoni, R. Tatarek, and G. Bracco, *Rev. Sci. Instrum.* **73**, 4257 (2002).
- ³⁰G. Bracco, R. Tatarek, F. Tommasini, U. Linke, and M. Persson, *Phys. Rev. B* **36**, 2928 (1987).
- ³¹J.W.M. Frenken and B.J. Hinch, *Helium Atom Scattering from Surfaces*, Springer Series in Surface Science, Vol. 27 (Springer-Verlag, Berlin, 1992), p. 287.
- ³²A.C. Levi and H. Suhl, *Surf. Sci.* **88**, 221 (1979).
- ³³G. Armand and J.R. Manson, *Phys. Rev. Lett.* **43**, 1839 (1984).
- ³⁴J.L. Beeby, *J. Phys. C* **4**, L359 (1971).
- ³⁵G. Boato, *Atomics and Molecular Beam Methods* (Oxford University Press, New York, 1992), Vol. 2, p. 340.
- ³⁶A. Luntz, L. Mattered, M. Rocca, F. Tommasini, and U. Valbusa, *Surf. Sci.* **120**, L447 (1982).
- ³⁷R. Ferrando (private communication).

- ³⁸D.P. Jackson, Surf. Sci. **43**, 431 (1974).
- ³⁹G. Bracco, A. Pizzorno, and R. Tatarek, Surf. Sci. **377/379**, 94 (1997).
- ⁴⁰C. Waldfried, D.N. McIlroy, J. Zhang, P.A. Dowben, G. Katrich, and E. Plummer, Surf. Sci. **363**, 296 (1996).
- ⁴¹B. Gumhalter, Phys. Rep. **351**, 1 (2001).
- ⁴²J.S. Ozcomert, W.W. Pai, N.C. Bartelt, and J.E. Reutt-Robey, Surf. Sci. **293**, 183 (1993).
- ⁴³J. Li, R. Berndt, and W.D. Schneider, Phys. Rev. Lett. **76**, 1888 (1996).
- ⁴⁴A. Trayanov, A.C. Levi, and E. Tosatti, Surf. Sci. **233**, 184 (1990).